Controlling the Inverted Pendulum

Steven A. P. Quintero
Department of Electrical and Computer Engineering
University of California, Santa Barbara
Email: squintero@umail.ucsb.edu

Abstract

The strategies involved in swinging up and balancing the inverted pendulum are discussed. The nonlinear swing-up controller drives the system input according to the energy of the pendulum. The balancing controller is a digital linear quadratic regulator that is based on a model of the plant that has been linearized about the pendulum's upright equilibrium position. Relays with hysteresis are employed to ensure smooth transitions between the two controllers.

1 Overview

The inverted pendulum is a classical problem that embodies numerous control theory topics. Thus, the purpose of this project is to investigate the nonlinear dynamics of the inverted pendulum experiment. In this case, the Quanser equipment will be used for both the purposes of design and testing. Figure 1 displays a diagram of the inverted pendulum system. The ultimate goal of the project is to design a controller that will swing the pendulum from its downward position of $\theta = \pi$ to its upright position of $\theta = 0$ and maintain that final angle. In addition, the cart should return to the center of the track, which allows free travel over a 0.8-m range. The methodology and results of the experiment are presented in this paper.

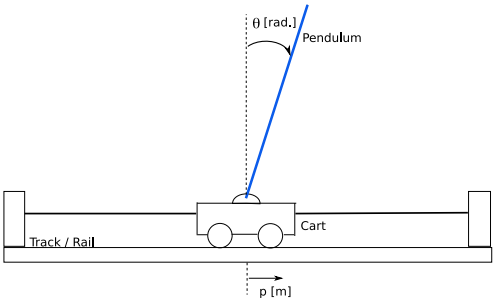

Figure 1: **Quanser Pendulum System**

2 Pendulum Dynamics

Since modern control methods are being used, the state equations must be derived from the governing set of differential equations for the system. The general dynamics of the system are presented in the free body diagram (FBD) depicted in Figure 2. Using the laws of Newtonian dynamics on the FBD, one can obtain the required set of differential equations. In Figure 2, the force of the dc motor on the cart is denoted by F. The equal and opposite forces that occur between the cart and the free-turning pendulum are labeled as N and P. The force that the track exerts on the cart is R while the gravitational forces on the pendulum and the cart are the terms $m_p g$ and $m_k g$, respectively.

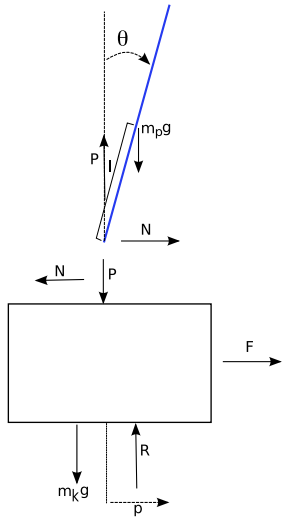

Figure 2: **Pendulum System Free Body Diagram**

The system has several parameters associated with its components that are required for determining the differential equations; they are described in Table 1. The force the dc motor exerts on the cart is dependent on the input voltage and the velocity of the cart, and the relationship is

$$F = \frac{K_m K_g}{Rr} V - \frac{K_m^2 K_g^2}{Rr^2} \dot{p}. \tag{1}$$

Parameter	Term	Units
DC Motor Torque Constant	K_m	$\frac{Nm}{Amp}$
Gearbox Gearing Ratio	K_g	N/A
Motor Armature Restistance	R	Ω
Motor Pinion Radius	r	m
Half-Length of Pendulum	ℓ	m
Cart Mass	m_k	kg
Pendulum Mass	m_p	kg
Rotational Inertia	I	kg m^2

Table 1: System Parameters

Several terms appear frequently in the system differential equations, and thus the following terms are defined for conciseness: $M = m_k + m_p$ and $L = \frac{I+m_p\ell^2}{m_p\ell}$. Also, define the state vector, $\vec{x} \in \mathcal{R}^4$, as follows:

$$\begin{pmatrix} x_1 & x_2 & x_3 & x_4 \end{pmatrix}^T = \begin{pmatrix} p & \dot{p} & \theta & \dot{\theta} \end{pmatrix}^T. \quad (2)$$

By utilizing the given information, one can derive the state equations, with the dc motor voltage as the only system input. Since the applied controls techniques and their results are the focus of this paper rather than the mechanical principles, the exact details of the derivation are not shown. The nonlinear state equations are given as Equations 3-6 for the purpose of verification.

$$\dot{x_1} = x_2 \quad (3)$$

$$\dot{x_2} = \left(M - \frac{m_p\ell\cos^2 x_3}{L}\right)^{-1}\left[\frac{K_mK_g}{Rr}V - \frac{K_m^2K_g^2}{Rr^2}x_2 - \frac{m_p\ell g\cos(x_3)\sin(x_3)}{L} + m_p\ell x_4^2\sin x_3\right] \quad (4)$$

$$\dot{x_3} = x_4 \quad (5)$$

$$\dot{x_4} = \left(L - \frac{m_p\ell\cos^2 x_3}{M}\right)^{-1}\left[\frac{\cos x_3}{M}\left(\frac{K_m^2K_g^2}{Rr^2}x_2 - \frac{K_mK_g}{Rr}V\right) + g\sin x_3 - \frac{m_p\ell x_4^2\cos(x_3)\sin(x_3)}{M}\right] \quad (6)$$

For the parameter values and a detailed method on obtaining the differential equations, please refer to [1].

3 Swing-Up

The swing-up methodology is based on the energy of the pendulum, and according to [2], the performance of the swing-up is based on the ratio of the maximum acceleration of the pivot to the acceleration of gravity (g). When discussing swing-up behavior, the term *performance* is generally used to denote the minimum number of swings required to attain the upright position of $\theta = 0$; however, the approach that is actually employed seeks robust system performance and does not exploit the cart's maximum accleration.

We now investigate a control law which will continuously inject energy into the system according to the strategy provided provided by [2]. The motion and energy (for $\ddot{p} = 0$) equations of the pendulum are as Equations 7 and 8, respectively,

$$J\ddot{\theta} - m_pg\ell\sin\theta = -m_p\ddot{p}\ell\cos\theta \quad (7)$$

$$E = \frac{1}{2}J\dot{\theta}^2 + m_pg\ell(\cos\theta - 1). \quad (8)$$

Note that J is the moment of inertia with respect to the pivot, as opposed to I, which is the moment of inertia with respect to the pendulum's center of mass. Also, the energy of the upright position is zero, and this is the desired system energy. Using Equations 7 and 8, one can compute the derivative of E with respect to time, which is

$$\frac{dE}{dt} = \dot{E} = J\dot{\theta}\ddot{\theta} - mg\ell\dot{\theta}\sin\theta = -m\ddot{p}\ell\dot{\theta}\cos\theta. \quad (9)$$

To have the system converge to E = 0, the control law given by Equation 10 is used with k positive and the *sign* function defined by Equation 11.

$$\ddot{p} = kE\text{sign}(\dot{\theta}\cos\theta) \quad (10)$$

$$\text{sign}(\phi) = \begin{cases} 1 & \text{if } \phi \geqq 0 \\ -1 & \text{else} \end{cases} \quad (11)$$

We show this works by a Lyapunov approach. If the Lyapunov function is given by Equation 12, then its time derivative is given by Equation 13.

$$V = \frac{1}{2}E^2 \quad (12)$$

$$\dot{V} = E\dot{E} = -mk\ell E^2\dot{\theta}\cos\theta\text{sign}(\dot{\theta}\cos\theta) \quad (13)$$

From the equation for $\dot{V}$, one can see that the derivative is negative semidefinite, and hence E will tend to zero so long as $\dot{\theta} \neq 0$ and $\cos\theta \neq 0$. Note that $\theta = \dot{\theta} = 0$ implies $\ddot{p} = -2kmg\ell$, which entails that the cart will experience an initial acceleration from rest and be forced out of the downward equilibrium position. Thus, since $\dot{\theta}$ cannot remain identically zero nor θ remain at $\pm\pi/2$, the system will converge to E = 0.

In order to demonstrate the effectiveness of the swing-up algorithm, a simulation was performed in *MATLAB*. The results of the simulation are shown

in Figure 3, and the computations employ the dynamics of Equations 3-6 and the control law of Equation 10 with $k = 10$. From this plot, one can see that the energy monotonically increases to zero as the pendulum nears the desired angle.

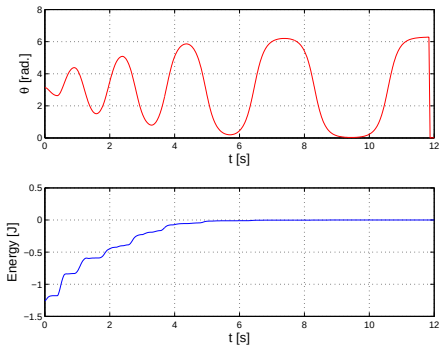

Figure 3: **Pendulum Angle and Energy**

Up to this point, a few details have been neglected and will now be discussed. The parameter k is an empirically-determined coefficient that determines how fast the swing-up controller will drive the pendulum to the upward position. Also, the required accelerations for swing-up have not been translated into the actual voltage input; however, this is done by rearranging Equation 4 to solve for the voltage in terms of the acceleration and other states. In addition, a full knowledge of the states has been assumed, though only θ and p are measured. In order to address this, the measured signals of θ and p are passed through Butterworth lowpass filters with cutoff frequencies of 20 and 25 rad/s, respectively. After this removal of high frequency noise, the derivatives of these signals are taken to yield the required states for the swing-up controller. Please note that this is not done in the case of upright stabilization, which uses the estimated states of a linear observer.

4 Upright Stabilization

With the state equations, it would be desirable to apply linear system theory to stabilize the pendulum in the upright position. As mentioned earlier, the system is inherently nonlinear. The solution has thus been to linearize the system about $\vec{x} = 0$. Thus, we compute the Jacobian A and B matrices from the nonlinear state equations and evaluate at the desired operating point. Finally, the C and D matrices convey the information that x_1 and x_3 are the outputs with no direct feedforward path from the input to the output.

Thus far the system has been treated as being continuous while in fact the use of the Quanser I/O boards and the Simulink Real-Time Workshop implies that it is actually discrete. Therefore, in order to properly design a controller, we calculate the zero-order hold equivalent of the linearized system, where a sampling period of $T_s = 1\ ms$ is used. The poles of the resultant system are located at $z = \{1,\ 0.984,\ 1.005,\ 0.995\}$. Since modern control techniques are to be applied, we first calculate the controllability and observability matrices, and they fortunately both have full rank, which implies that the system is both controllable and observable. With these properties, we are now assured that state feedback can be used to stabilize the system, even though all of the states are not measured.

Instead of a standard pole placement approach, we use a linear quadratic regulator (LQR) in order to limit the amount of energy expended by the system and avoid overly large state feedback gains. The R and Q parameters involved with the computation are determined by imposing heavier penalties on p and θ and through experimentation. The tuned parameters are given as Equations 14 and 15.

$$R = 1 \tag{14}$$

$$Q = diag(\begin{bmatrix} 25 & 10 & 50 & 0.1 \end{bmatrix}) \tag{15}$$

The state feedback gains resulting from the use of such parameters are K = [-4.96 -12.3 -34.9 -6.77], and the new closed-loop poles are located at $z = \{0.981,\ 0.993,\ 0.997,\ 0.999\}$. The system clearly does not have fast dynamics, though it is stable within a certain neighborhood of the origin and expends a reasonable amount of energy.

State feedback naturally assumes a knowledge of all states, though only two of the four states are actually measured. In order to remedy this problem, we design a linear state estimator to provide the rest of the required information. As the system dynamics are not quick, we place the closed-loop estimator poles at $z = \{0.85,\ 0.90,\ 0.95 \pm 0.05\jmath\}$. Finally, we model the $\pm$5V limits of the dc motor as saturation to the input of the state estimator in order that the estimated states abide by such a constraint.

5 Controller Unification

The main parameters for switching from one controller to another are θ and $\dot{\theta}$, and these parameters must be chosen so that switching from the swing-up controller to the upright stabilization controller does not result in saturation of the input voltage signal. In addition, rapid switching back and forth between the two controllers, or chattering, must be avoided. Thus, in order to avoid such chattering, a logic relay with hysteresis is used, as depicted in Figure 4. Thus, the output of this relay is a digital

logic signal, which is based on the manner in which the input signal passes through S^- and S^+. Since there are two such hysteresis loops, the outputs are passed through a logical *or* gate. Table 2 describes the empirically determined parameters for each of the hysteresis loops, and note that the measurement of θ has been slightly altered, as $\theta \in (-\pi, \pi]$.

Hysteresis Input	$\mathbf{S^-}$	$\mathbf{S^+}$
$\lvert\theta\rvert$ [rad.]	0.07	0.2
$\lvert\dot{\theta}\rvert$ [rad./s]	1.3	1.5

Table 2: Hysteresis Parameters

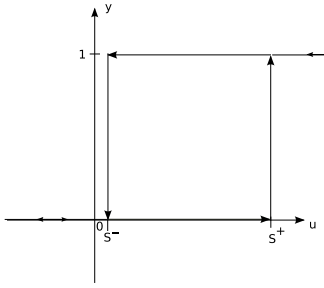

Figure 4: **Logic Relay with Hysteresis** - Outputs a binary value (y) according to how the input (u) crosses S^- and S^+

From the information of Table 2, we see that if $|\theta| < 0.07$ and $|\dot{\theta}| < 1.3$, then both relays will output logic values of zero. When these two values are passed through the *or* gate, the output will also be zero; consequently, it is this logic value that is required for the upright stabilization controller to assume control authority. Conversely, if at least one relay outputs a logical one, then the output of the *or* gate will be one as well. In this case, the swing-up controller retains control authority. Moreover, the use of two logic relays with hysteresis and a logical *or* gate has allowed for smooth changes between controllers.

6 Avoiding Track Edges

In order to prevent the cart from hitting the ends of the track, a penalty is imposed on the original desired accelerations of the swing-up controller. Thus, according to the strategy proposed by [3] , Equation 10 now becomes the following:

$$\begin{aligned} \ddot{p} &= kE\text{sign}(\dot{\theta}\cos\theta) \\ &\quad + \frac{5}{2}\arctan\left(\frac{p}{0.4}\right)\ln\left(1 - \frac{|p|}{0.4}\right). \end{aligned} \quad (16)$$

Based on Equation 16, the swing-up controller will keep the cart away from the ends of the track ($|p| = 0.4$), since heavy penalties are incurred near such locations. Moreover as the cart moves close to one end of the track, the swing-up controller will demand an acceleration towards the center of the track and thereby output the appropriate voltage.

Sometimes the situation arises when the upright stabilization controller will catch the pendulum as the cart is near the edge of the track and drive the cart further toward that edge. In order to such a dangerous situation, an additional logic relay with hysteresis has been added to the logical *or* gate that was mentioned in §5. This hysteresis loop takes $|p|$ as an input and has S^- and S^+ set at values of 0.33 and 0.38, respectively. Moreover, if the cart goes beyond 0.38 $[m]$, the swing-up up controller will seize control authority until the cart has returned to within 0.33 $[m]$ of the track's center and both constraints on θ and $\dot{\theta}$ are met according to Table 2.

7 Results

In order to test the system, the cart is centered on the track and the pendulum is stabilized in the downward position. The controller is then engaged in Simulink, and the results from one such test are presented in Figures 5 and 6. During this test, the swing-up controller takes the pendulum from rest to the upright position in just over 13 seconds, after which the upright stabilization controller seizes control authority and catches the pendulum. Notice how the cart stays within 0.3 $[m]$ of the track's center.

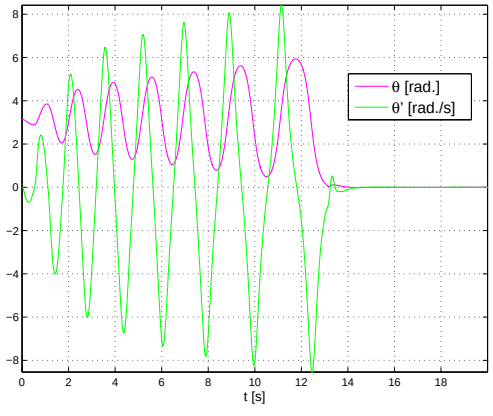

Figure 5: **Pendulum Angle and Velocity**

From the second subplot in Figure 6, we see that the voltage saturates only for small amounts of time as the swing-up controller is close to achieving its goal. When the digital LQR controller is switched on, the voltage still remains well within the limits of

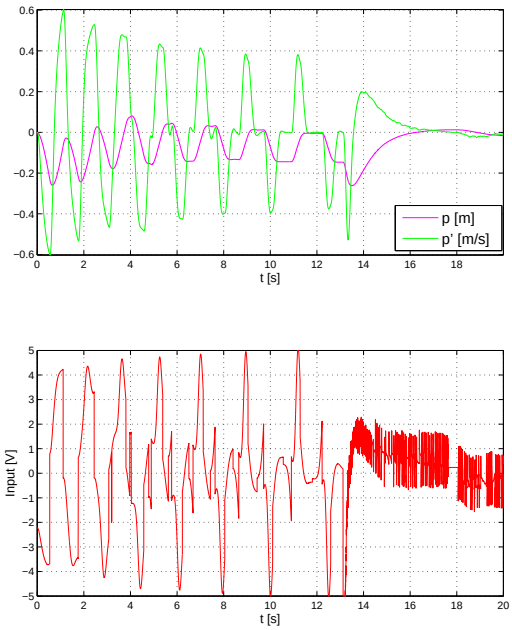

Figure 6: **Cart Position and Motor Input**

the dc motor. It must be mentioned, however, that during this test the incorrect value for pendulum's moment of inertia with respect to its pivot was used to compute the pendulum's kinetic energy. In this case, I was used instead of J, where $J = 4I$. Had this error been discovered earlier, more tests could have been run with the correct value and the actual energy plotted. Note that the simulation of Figure 3 uses the correct value for J. Regardless of this miscalculation, the goal of swinging up the pendulum was achieved.

The pendulum is also robust at rejecting disturbances, and this is illustrated in Figure 7. The digital LQR controller is able to reject small disturbances, as shown in the first 15 seconds of the plot. Also, if a disturbance knocks the pendulum beyond the upright stabilizing controller's region of attraction, the swing-up controller assumes control authority and brings the pendulum back up to the desired angle. This latter form of disturbance rejection is shown during the time interval of 19 to 37 seconds.

8 Concluding Remarks

The swing-up controller performs desirably, though a few unfortunate traits have been noted. In a few instances, the pendulum will come up with an excessive angular velocity and not allow the upright stabilization controller to assume authority as the

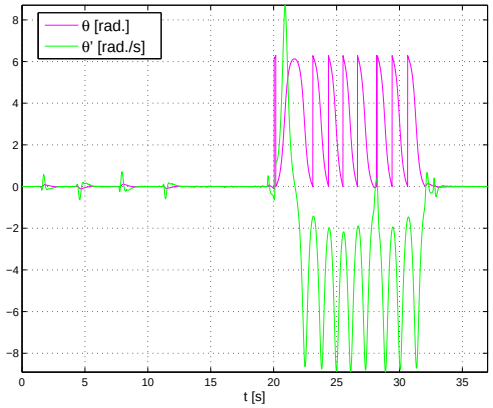

Figure 7: **Disturbance Rejection**

pendulum passes through the desired angle. When this occurs, the pendulum will be repeatedly swung about the pivot until the cart nears the end of the track, at which point the pendulum will begin to lose energy according to the penalty of Equation 16 and ultimately satisfy the transition constraints. Thus, this situation simply results in extra swings of the pendulum. Also, the performance of the swing-up controller changes as plant parameters are varied slightly; thus, the controller must be tuned by changing the value of k each time a different Quanser inverted pendulum system is used.

As for the remaining project components, the digital LQR controller yields satisfactory performance, since it is able to stabilize the pendulum in its upright position and reject small disturbances. This controller is also robust with respect to slight plant variations. The use of relays with hysteresis to switch between the two controllers prevents chattering from occurring and therefore behaves as required. Moreover, two controllers have been successfully designed, implemented, and united for the purposes of swinging up the pendulum from rest to its upright position and maintaining that angle.

References

[1] Smith, Roy. *Lab 3: Balancing the Inverted Pendulum.* ECE147b: Digital Control. `http://www.ece.ucsb.edu/~roy/classnotes/147b/lab3_v2.pdf`

[2] Åstrom, Karl, and Katsuhisa Furata. *Swinging up a pendulum by energy control.* Automatica 36 (2000): 287-295.

[3] *Jägerhök*, Jonas. *Swinging and Controlling the Pendulum.* `http://www.ece.ucsb.edu/~roy/cgi-bin/makepage.pl?nav=projects`